Classical Monte Carlo simulation

Lukas Helmig

April 2023

1 Theory assignments

Considering the definition of the specific heat c_V, what quantity that is a function of the microscopic configurations can you use to compute c_V in a Monte Carlo simulation?

Since the heat capacity is defined as the temperature gradient from the expectation value of the energy

$$c_V = \frac{1}{V}\frac{\partial}{\partial T}\langle E\rangle, \tag{1}$$

we can insert the definition of the thermodynamic expectation value

$$c_V = \frac{1}{V}\frac{\partial}{\partial T}\left(\frac{1}{Z_\beta}\sum_{\underline{s}} H(\underline{s})\exp\left(-\frac{H(\underline{s})}{T}\right)\right). \tag{2}$$

When one now computes the derivative, the fluctuation-dissipation theorem for the energy is obtained

$$c_V = \frac{1}{VT^2}(\langle E^2\rangle - \langle E\rangle^2) \tag{3}$$

What is the entropy of the frustrated magnet at infinite temperature ($\beta = 0$)?

The Boltzmann entropy is given by

$$S = k_B = \ln(\Omega(E)), \tag{4}$$

where Ω is the number of microstates in an interval $E + dE$. For $\beta \to 0$, every microstate is accessible, which amounts to $\Omega = 2^n$ for n spins on a lattice. Then an entropy of

$$S = k_B \ln(2^n) = k_B n \ln(2) \tag{5}$$

is obtained. In the actual simulations, we set $k_B = 1$.

Assuming that you know the specific heat as a function of temperature, $c_V(T)$, how can you determine the entropy at $T = 0$?

As the entropy is a function of state, it can be calculated through a line integral in the thermodynamic state space

$$S(T=0) = S(T=\infty) + \int_\infty^0 \frac{\delta Q_{\text{rev}}}{T}. \tag{6}$$

Since the amount of heat can be expressed with the specific heat $\delta Q_{\text{rev}} = c(T)dT$, the residual entropy can be calculated via

$$S(T=0) = S(T=\infty) + \int_\infty^0 \frac{c(T)}{T}dT. \tag{7}$$

Convince yourself that the Metropolis-Hastings acceptance probability fulfills the detailed balance condition.

The detailed balance condition is given by

$$\pi(s)p_{\text{mc}}(s \to s') = \pi(s')p_{\text{mc}}(s' \to s). \tag{8}$$

For the Metropolis-Hastings algorithm, the transition probability is

$$p_{\text{mc}}(s \to s') = p_{\text{p}}(s'|s)p_A(s, s'). \tag{9}$$

Inserting this into detailed balance, we obtain

$$\frac{\pi(s)p_p(s'|s)}{\pi(s')p_p(s|s')} = \frac{p_{\text{a}}(s', s)}{p_{\text{a}}(s, s')} = \frac{\min\left(1, \frac{\pi(s)p_p(s'|s)}{\pi(s')p_p(s|s')}\right)}{\min\left(1, \frac{\pi(s')p_p(s|s')}{\pi(s)p_p(s'|s)}\right)}.$$

After making a simple case distinction with $\pi(s)p_p(s'|s) > \pi(s')p_p(s|s')$, it is immediately seen that detailed balance holds.

2 Ferromagnet

Determine a suited grid for the temperature axis - (3.1.1)

First, we need to determine a suitable temperature grid. In figure 1, the results of a Monte-Carlo simulation with an evenly spaced temperature grid with steps $\Delta T = 0.1$ are illustrated. The chosen

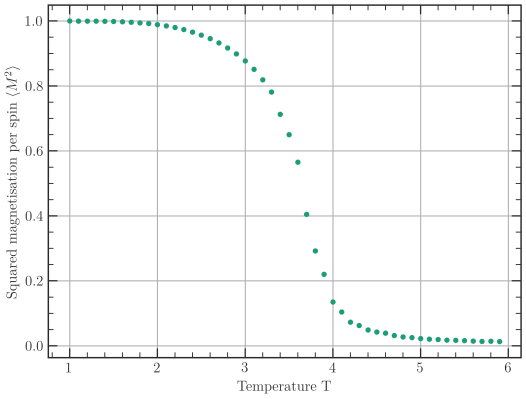

Figure 1: Squared magnetization $\langle M^2 \rangle$ depending on the temperature ($L = 20$, $n_{\text{samples}} = 20000$). Temperature ranges from 0 to 6 with steps of $\Delta T = 0.1$.

temperature grid seems to be depicting the phase transition reasonably well, which means that the chosen grid is sufficient. However, one can decrease the spacing between temperatures 3.4 and 3.8, if necessary.

Compute and plot the autocorrelation function $\gamma(t)$ - (3.1.2)

The auto-correlation function of the squared magnetisation per site and the energy per site can be seen in figure 2 and 3. From now on, we denote the number of attempted spin flips per sweep with n_{sweep}. It is seen that the auto-correlation function

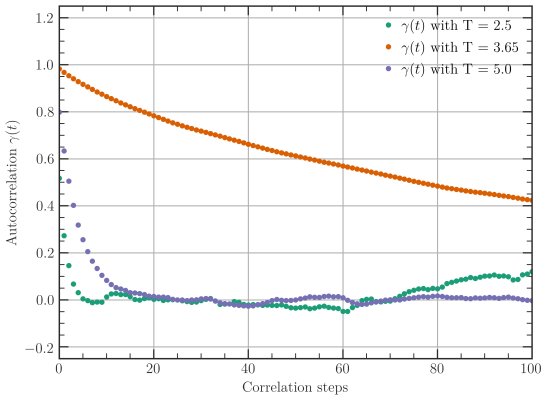

Figure 2: Autocorrelation of the squared magnetisation per site $\langle M^2 \rangle$, computed for temperatures 2.5, 3.65 and 5. ($L = 40$, $n_{\text{samples}} = 20000$, $n_{\text{sweep}} = L^2$)

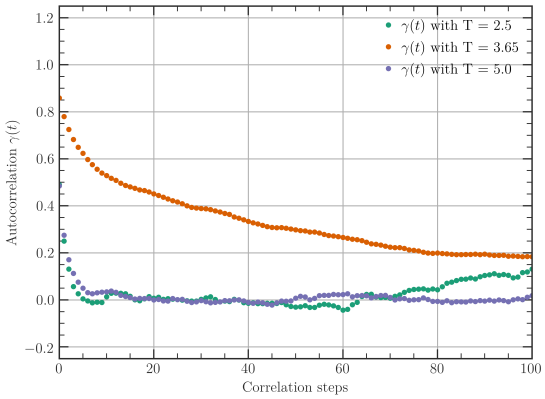

Figure 3: Autocorrelation of the energy per site $\langle E \rangle$, computed for temperatures 2.5, 3.65 and 5. ($L = 40$, $n_{\text{samples}} = 20000$, $n_{\text{sweep}} = L^2$)

for both magnetisation and energy at $T = 3.65$ is decaying on a very slow scale. Of course, this makes sense, since the temperature is close to the critical

temperature of the phase transition. At the phase transition, the correlation length diverges producing a slow decay of the auto-correlation. For the other two temperatures, the observables decay much faster. It can also be noticed that at temperature $T = 2.5$ the auto-correlation is smaller compared to $T = 5$. This a bit surprising, since one would generally suspect that sequential states are less correlated for higher temperatures.

Convince yourself that the sequence of error estimates of the binning analysis converges as function of the coarse-graining size k - (3.1.3)

In figure 4, the error estimate is plotted depending on the binning size k. The temperature is chosen to be close to the phase transition. It can be very

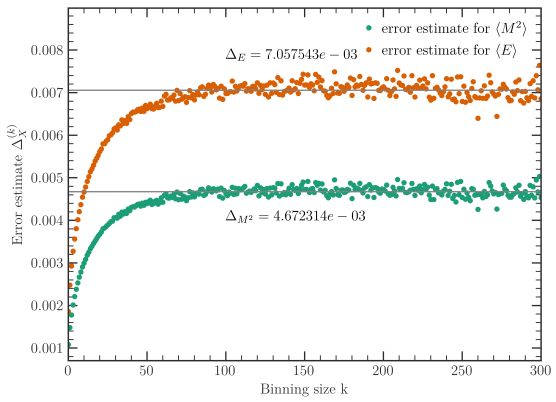

Figure 4: Error estimate of the binning analysis for $\langle M^2 \rangle$ and $\langle E \rangle$ ($L = 10$, $T = 3.65$, $n_{\text{sweep}} = L^2$).

clearly seen that the error estimate konverges, when the binning size k is increased. For other system sizes and temperatures, the converging behavior remains the same. It might be that one has to increase the binning size k until convergence is achieved.

Compute the expectation values of the squared magnetization - (3.1.4)

Figure 5 is showing the expectation value of the magnetisation for different temperatures. At lower

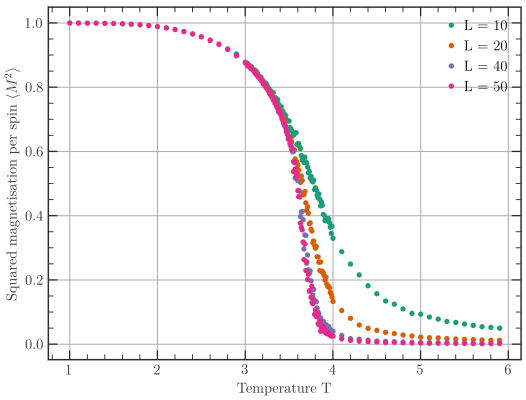

Figure 5: Temperature dependent expectation value of the squared magnetization $\langle M^2 \rangle$ for various system sizes.($L = 10$, $T = 3.65$).

temperatures, all spins point in the same direction with an average magnetisation of ≈ 1 per site. At higher temperatures, the average magnetisation is 0, each spin can align freely. Between the low and the high temperature regime, there is a phase transition, which can be seen at approx. $T = 3.7$ for all system sizes. With larger system sizes, the transition gets sharper with the limit being a discontinuous jump.

Compute the specific heat for all system sizes as function of temperature - (3.1.5)

The specific heat as a function of temperature can be seen in figure 6. The specific heat shows a peak at the critical temperature and decreases for lower and higher temperatures. By plotting the unscaled specific heat, one obtains the so called scaling-collapse, figure 7.

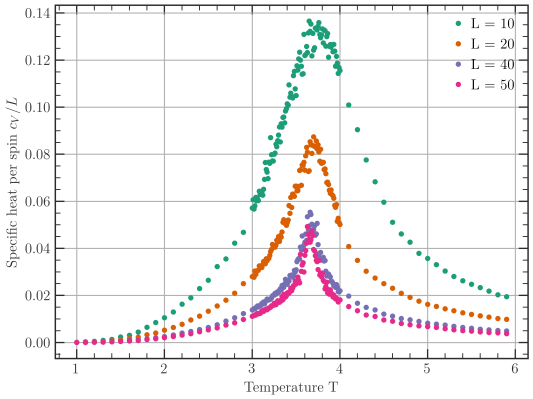

Figure 6: Scaled specific heat c_V/L as a function of temperature for various system sizes ($n_{\text{samples}} = 20000$).

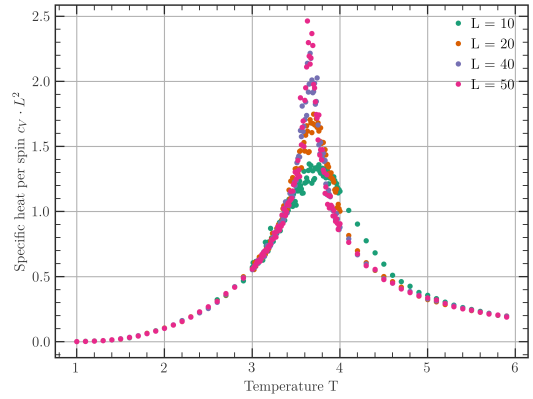

Figure 7: Scaling collapse of the specific heat.

3 Antiferromagnet

Convince yourself that the sequence of error estimates of the binning analysis converges as function of the coarse-graining size k - (3.2.6)

Figure 8 shows the convergence of the error estimate exemplary for $\langle M^2 \rangle$ for a small system size of $L = 10$ at two temperatures. For other system sizes and temperatures, a convergence can also be found.

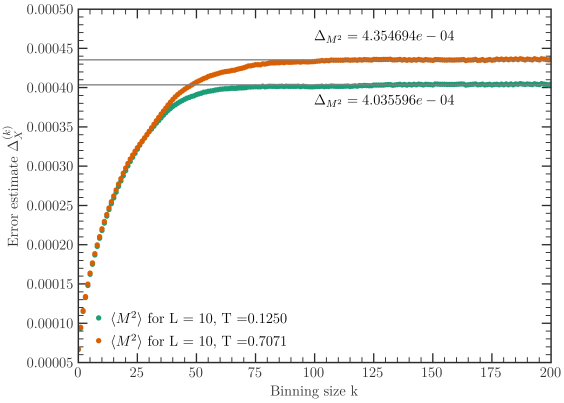

Figure 8: Error estimate of the binning analysis for $\langle M^2 \rangle$, exemplary for system size $L = 10$, $T \approx 0.7071$) and $T = 0.125$ ($n_{\text{samples}} = 50000$, $n_{\text{sweep}} = 1$)

Figure 9 shows the auto-correlation of the squared magnetisation and energy. It is seen that the auto-correlation increases with system size. We expect a lower auto-correlation time with increasing temper-

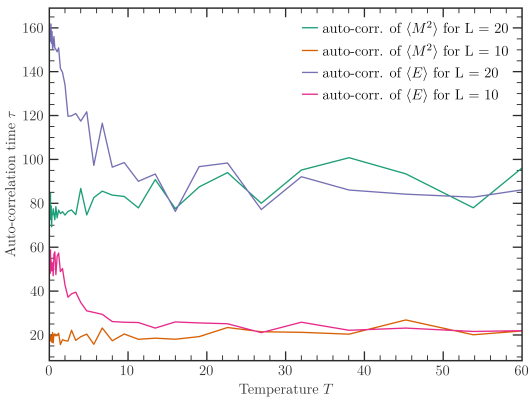

Figure 9: Auto-correlation of $\langle M^2 \rangle$ and $\langle E \rangle$ as a function of temperature T

ature, which is found for the energy. However, the squared magnetisation shows actually an increase of the auto-correlation with temperature, for which the reason is not apparent.

Compute the specific heat as function of temperature for each system size. Compare the behavior to your results for the ferromagnet. - (3.2.7)

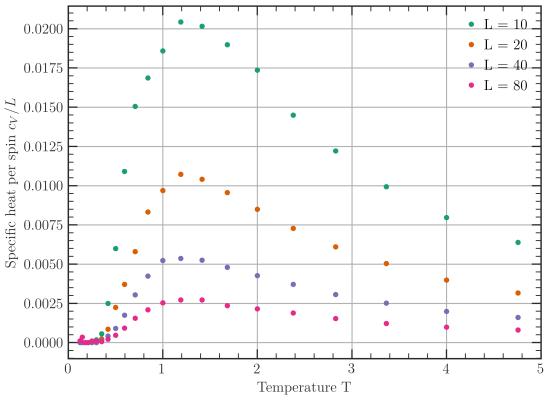

Figure 10: Scaled specific heat c_V/L as a function of temperature for various system sizes ($n_{\text{samples}} = 20000$).

Figure 10 shows the scaled specific heat c_V/L as a function of temperature. Just as in the ferromagnetic case, the specific heat assumes a maximum at a temperature of $T \approx 1.1$. However, this maximum is totally continuous and does not form a sharp peak. It can be seen that there is no phase transition in the antiferromagnetic case. The specific heat decreases below and above the temperature of the maximum. For temperatures $T \to 128$, the specific heat goes to 0.

Using the specific heat, compute the zero-point entropy of the frustrated magnet. How does the value you find compare with the exact value from the literature? Discuss possible deviations. - (3.2.8)

Using `integrate.simpsons()` from `SciPy` to numerical integrate the specific heat, we obtain the residual entropy by subtracting the integrated specific heat from the entropy at $T = \infty$. The result is seen in figure 11. It is seen that we underestimate

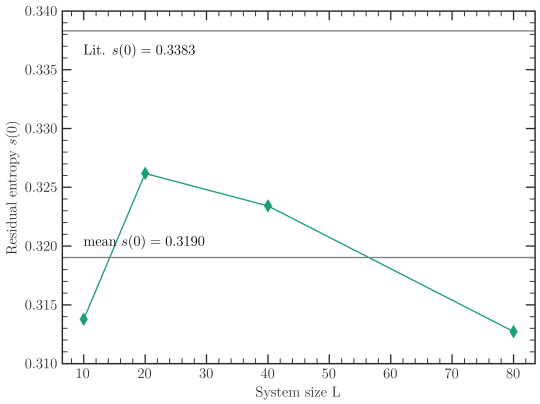

Figure 11: Residual entropy for system sizes $L = 10, 20, 40, 80$.

the literature value for the residual entropy, meaning that we overestimate the integral over the specific heat. There is also no clear trend for larger system sizes. The deviation from the literature value could stem from the inaccuracy of the numerical integration, finite-size effects or statistical fluctuations.

Generate samples for a grid of magnetic field values $B \in [0, 10]$. Compute the magnetization as a function of the magnetic field. - (3.2.9)

Figure 12 shows the magnetization for an increasing magnetic field. It can be observed that the magnetization does not increase monotonically, but saturates at magnetic fields $h \geq 6$. At some point, the strength of the magnetic field outweighs the energy penalty from the antiferromagnetic interactions. Therefore, the spins will align in the same direction despite the antiferromagnetic interaction.

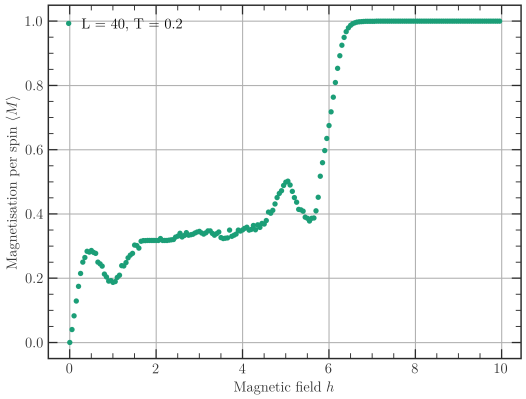

Figure 12: Magnetization per site $\langle M^2 \rangle$ for $T = 0.2$ and $L = 40$ as a function of the magnetic field $0 \leq h \leq 10$.

Figure 13 shows the average energy per site as a function of the magnetic field. As one can see, the energy steadily decreases with a higher magnetic field. This is as expected, because the magnetic field

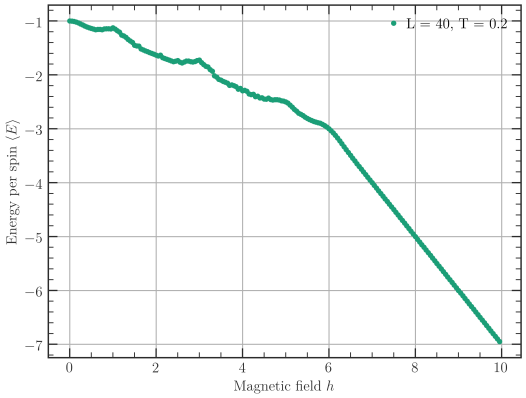

Figure 13: Energy per site $\langle E \rangle$ for $T = 0.2$ and $L = 40$ as a function of the magnetic field $0 \leq h \leq 10$.

forces more and more neighbouring spins to align parallel. Since the interaction is antiferromagnetic, the energy decreases.

Calculate the spin-spin correlation function along a horizontal cut in the lattice. - (3.2.10)

The correlation of two spins along a horizontal cut in the lattice can be seen in figure 14. For a temperature $T = 1$, there is basically no spin correlation. When looking at a low temperature of $T = 0.1$, it is seen that the correlation is generally decaying over a larger real space distance. But one can notice that

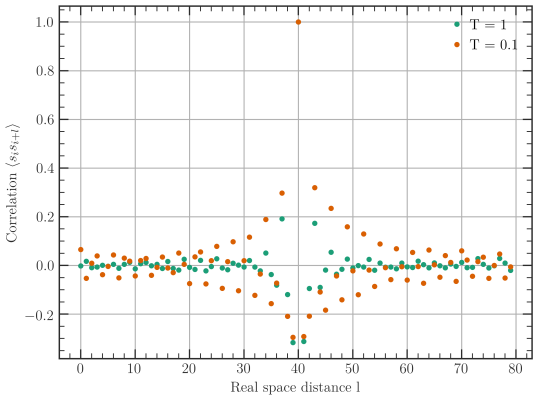

Figure 14: Spin correlation $\langle s_i s_{i+l} \rangle$ as a function of the site index l along a horizontal cut. The system size is $L = 80$, $n_{\text{samples}} = 20000$.

the next neighbour is positively correlated, but the next-next neighbour negatively. This is due to the anti-ferromagnetic interaction. At some sites, a vanishing correlation is observed. This can be explained with magnetic frustration, because the spin at that site has the same number of satisfied and dissatisfied bonds and can therefore align freely in each direction.

4 Issues

Changing the number of sweeps from L^2 to 1 in figure 2 and 3 leads to $T = 5.0$ having the highest auto-correlation instead of $T = 3.65$ close to the phase transition.

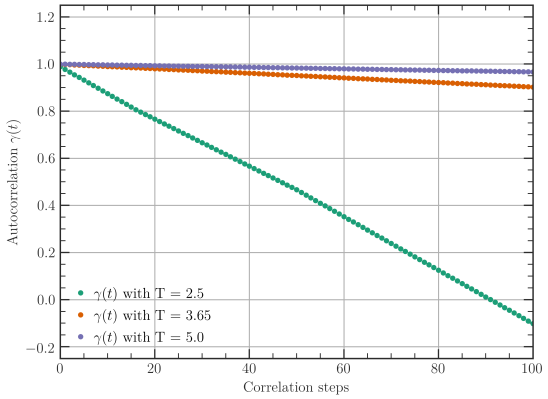

Figure 15: Autocorrelation of the squared magnetisation per site $\langle M^2 \rangle$, computed for temperatures 2.5, 3.65 and 5. ($L = 40$, $n_{\text{samples}} = 20000$, $n_{\text{sweep}} = 1$)

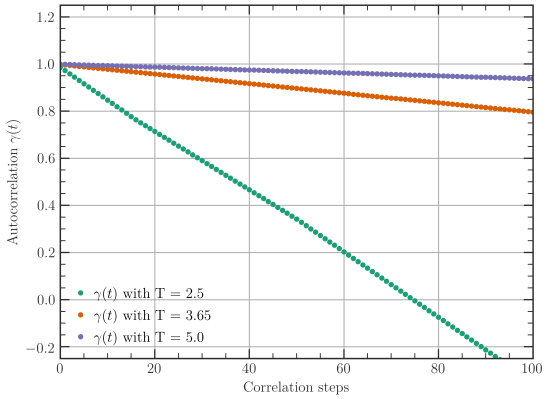

Figure 16: Autocorrelation of the energy per site $\langle E \rangle$, computed for temperatures 2.5, 3.65 and 5. ($L = 40$, $n_{\text{samples}} = 20000$, $n_{\text{sweep}} = 1$)

The auto-correlation time of the squared magnetisation in figure 9 increases with temperature, which was not expected.